

Substrate Driven Photochemistry of CdSe Quantum Dot Films: Charge Injection and Irreversible Transformations on Oxide Surfaces[†]

Kevin Tvrdy and Prashant V. Kamat*

Radiation Laboratory, Department of Chemistry and Biochemistry, and Department of Chemical and Biomolecular Engineering, University of Notre Dame, Notre Dame, Indiana 46556

Received: September 26, 2008; Revised Manuscript Received: December 09, 2008

The photochemical behavior of CdSe quantum dots anchored to different surfaces was probed through their deposition on glass, SiO₂, and TiO₂ films. Following visible light irradiation under ambient conditions, CdSe quantum dots deposited on semiconducting TiO₂ surface degraded, where no such degradation was observed when deposited on inert SiO₂ surface or glass. Fluorescence decay and transient absorption experiments confirmed that charge injection from excited CdSe into TiO₂ occurs with an apparent rate constant of $5.62 \times 10^8 \text{ s}^{-1}$ and is the primary event responsible for photodegradation. In the presence of air, injected electrons are scavenged by surface adsorbed oxygen leaving behind reactive holes which induce anodic corrosion of CdSe quantum dots. In a vacuum environment, minimal CdSe degradation was observed as electron scavenging by oxygen is replaced with charge recombination between injected electrons and holes in CdSe nanocrystals. Spectroscopic measurements presented in this study highlight the role of both substrate and medium in dictating the photochemistry of CdSe quantum dots.

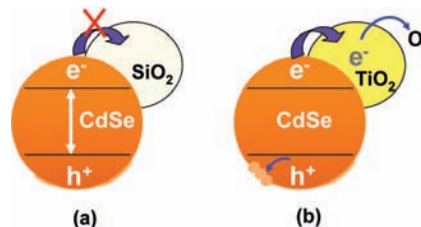
Introduction

Semiconductor quantum dots are extensively used as biological probes and as light harvesters.^{1–6} Because of their size dependent electronic and optical properties, quantum dots are often used as model systems to explore new phenomena related to nanotechnology.^{7–9} Of particular interest is the phenomenon of multiple charge carrier generation and its potential implementation in solar cells.¹⁰ Recent work from our laboratory^{11,12} and elsewhere^{13–17} has highlighted the use of quantum dots in solar cells. By anchoring different sized CdSe quantum dots on mesoscopic TiO₂ films, we succeeded in tuning the photoresponse of solar cells. The redox electrolyte employed in these cells allowed us to maintain long-term stability in such devices.

A major concern that arises in many of these studies revolves around the photostability of the sensitizers employed and the factors that dictate interfacial photochemistry (Scheme 1). In particular, such concerns are of great importance in single particle spectroscopy measurements,¹⁸ optoelectronic devices,¹⁹ and solar cells.²⁰ For example, to achieve accurate single particle measurements it is critical that the particle under investigation remain stable over long-term laser irradiation. Any interfacial interaction between quantum dots and the substrate they rest upon may significantly affect photophysical properties. Photoluminescence experiments carried out at high laser fluences (0.5–10 mJ/cm²) show that the photoluminescence decay depends on the nature of the surrounding matrix.²¹

To probe the interfacial charge transfer processes between semiconducting nanoparticles and the substrate to which they are anchored, we deposited 4.2 nm diameter CdSe quantum dots on both TiO₂ and SiO₂ substrates and subjected them to steady-state visible irradiation under both atmospheric and vacuum conditions. Time-resolved transient absorption and emission

SCHEME 1: Deactivation of Photogenerated Charge Carriers in CdSe Quantum Dots^a



^a (a) Radiative/nonradiative charge recombination when in contact with SiO₂. (b) Transfer of electrons from CdSe to TiO₂ followed by hole oxidation at the surface.

measurements, which highlight the resultant photochemical events, are presented herein.

Experimental Section

Optical Measurements. Absorption spectra were recorded using a Cary Bio 50 spectrophotometer. Emission spectra were recorded using an SLM-S 8000 spectrofluorometer. Emission lifetimes were measured using a Horiba Jobin Yvon single photon counting system with a diode (457 nm, 1 MHz repetition, 1.1 ns pulse width) excitation source. Transient absorption measurements were conducted using a Clark-MXR 2010 (775 nm, 1 mJ/pulse, fwhm = 130 fs, 1 kHz repetition) laser system coupled with detection software from Ultrafast Systems (Helios). The pump–probe (pump 95% of fundamental, frequency doubled to 387 nm; probe 5% of fundamental used to generate white light continuum) beams were incident on the quartz 2 mm path length sample holder (room temperature) at an angle < 10°. The probe beam was collected with a CCD spectrograph (Ocean Optics, S2000-UV-vis) providing a 450–800 nm data window. Typically 1000 excitation pulses were averaged to obtain a transient spectrum at a set delay time.

Vacuum Cell Setup. To conduct spectroscopic measurements in vacuum the film under investigation was placed inside of a

[†] Part of the “George C. Schatz Festschrift”.

* To whom correspondence should be addressed. E-mail: pkamat@nd.edu.

vacuum cell²² to which a vacuum of $\sim 5 \times 10^{-3}$ torr was applied for 3 h, after which the cell was sealed. A 10 mm \times 10 mm vacuum cell was used for degradation measurements in which a film could be placed at various angles, and a 2 mm cell was used for transient absorption measurements. Unless otherwise specified, all measurements were carried out under vacuum.

Steady-State Photoirradiation. Steady-state photolysis/degradation measurements were carried out by placing the sample slide inside of a 10 mm \times 10 mm quartz cell, which was either left open to atmospheric conditions or evacuated. The sample was oriented inside of the sample chamber of the UV-vis spectrophotometer such that the surface normal of the film was $\sim 45^\circ$ relative to the path of the UV-vis beam. Visible light irradiation was carried out by focusing a tungsten white light source (Oriel 60005 lamp with Oriel 68830 power supply, see profile in Supporting Information) directly on the sample film (0.85 W) at $\sim 45^\circ$ relative to surface normal, making a $\sim 90^\circ$ angle between the UV-vis beam and the white light used for degradation (experimental setup shown in Supporting Figure 2 of Supporting Information).

Materials. Titanium(IV) isopropoxide (Titanium Isopropoxide, Acros, 98+); acetonitrile (Fisher, HPLC grade); 2-propanol (Fisher, certified A.C.S.); tri-*n*-octylphosphine oxide (TOPO, Acros, 99%); *n*-tetradecylphosphonic acid (TDPA, PCI Synthesis); 1-dodecylamine (DDA, Alfa, 98+); selenium powder, -100 mesh (Se, Aldrich, 99.5%); cadmium oxide (CdO, Alfa, 99.998%); trioctylphosphine (TOP, Aldrich, 90%); (3-mercaptopropyl)-trimethoxysilane (MPS, Aldrich, 95%); 3-mercaptopropionic acid (MPA, Aldrich, 99+); acetic acid (Fisher, glacial); toluene (Fisher, HPLC grade); methanol (Fisher, laboratory grade); SiO₂ nanoparticles (Nalco 2327, diameter = 20 nm); and water (deionized, filtered) were used.

TiO₂ Nanoparticles. TiO₂ nanoparticles were synthesized as follows: 3.7 mL of titanium isopropoxide and 1.0 mL of 2-propanol were placed in a dropping funnel and added at ~ 1 drop/sec to a vigorously stirred solution of 25 mL water and 8 mL acetic acid. The resulting white precipitate-containing solution was refluxed for 1 h., cooled to room temperature, and refluxed again for 4 h. The resulting milky-white solution was loaded into an autoclave and subjected to 230 °C heating for 12 h. The solution was then concentrated via rotovap to 8 mL, which assuming 100% reaction yield, corresponds to 122 mg TiO₂/mL. Dropcast films from such solution analyzed under SEM showed particle sizes ranging from 12–16 nm in diameter.

CdSe Nanocrystals. Size quantized CdSe nanoparticles were synthesized as previously described.¹² In brief, CdO, TOPO, TDPA, and DDA were heated under nitrogen to which a mixture of TOP and 1 M TOPSe was injected. CdSe nanoparticle size grew with increased temperature. Quantum dots were washed with a mixture of methanol and toluene and dissolved in toluene for storage.

Linking CdSe Nanocrystals to TiO₂ Films (CdSe/MPA/TiO₂). Prior to film creation TiO₂ nanoparticle solution was sonicated for 30 min, after which 40 μ L was placed on a microscope slide and spread evenly across a 0.7 cm \times 1.8 cm area. The film was air-dried and annealed in a 400 °C oven for 2 h to ensure anatase crystal structure and burn off residual materials. The temperature was then lowered to 120 °C for 10 min. The hot films were placed directly into a 1 M 3-mercaptopropionic acid (MPA) in acetonitrile solution for 12 h to allow for attachment of linker molecules. The films were subsequently washed with acetonitrile and toluene and placed directly in CdSe nanoparticle solution ($\sim 8 \times 10^{-6}$ mol of dots/L)²³ for 48 h. Upon removal from the quantum dot solution the films were

washed with toluene to ensure chemical adsorption of the quantum dots onto the semiconducting surface and stored in the dark. Film thickness as measured with an Alpha Step surface profiler (Tencor) was determined to be $\sim 8 \mu$ m.

CdSe/MPS/SiO₂ Films. SiO₂ films were cast upon a 0.7 cm \times 1.8 cm area of a microscope slide through direct spray coating with a 1:2 solution of SiO₂ nanoparticles/water. Repeated steps of spraying and air drying yielded an 8 μ m film. Films were subjected to 400 °C heat treatment for 2 h. The temperature was then lowered to 120 °C for 10 min. The hot films were placed directly in a 0.20 M MPS in toluene solution for 1 h. Films were washed with toluene, placed directly in CdSe nanoparticle solution for 48 h, and processed in the same fashion as the CdSe/MPA/TiO₂ films.

CdSe Films. Films comprised of quantum dots deposited directly on glass were created by dropcasting a solution of CdSe quantum dots in toluene on a heated (~ 80 °C) glass microscope slide. This was repeated until significant coloration on the slide (Abs ~ 0.25) was observed. All films were stored in the dark.

Results and Discussion

Absorption Characteristics. Steady-state absorption and fluorescence measurements were carried out to verify the adsorption of CdSe quantum dots onto both TiO₂ and SiO₂ substrates, as well as the nature of the CdSe quantum dots dropcast directly on glass (Figure 1), which are hereafter referred to as CdSe/MPA/TiO₂, CdSe/MPS/SiO₂, and CdSe/Glass, respectively. As discussed elsewhere,^{24,25} the bifunctional linker molecules MPA and MPS facilitate deposition of CdSe onto the TiO₂ and SiO₂ surfaces, respectively. The 1S_{3/2}1S_e transition²⁶ at 562 nm seen in the CdSe quantum dot toluene solution is retained in the CdSe/MPA/TiO₂, CdSe/MPS/SiO₂, and CdSe/Glass films. Note that the baseline offset present in all three films is not due to absorption of the respective materials but rather from scattering effects, which are inherent when working with nanoparticle films of 5–10 μ m thickness. Likewise, similar emission characteristics exist between the CdSe particles in solution and those that have been adsorbed onto films. These similar absorption and emission features suggest that the optical and electronic properties exhibited by the quantum dots in solution, specifically electronic transitions and relative band energies, are preserved when these dots are adsorbed onto films. This retention of quantization properties, as well as the semitransparent nature of these films, makes these films promising candidates for the study of quantum dot/substrate interactions using transmission spectroscopy.

Pump-Probe Spectroscopy Measurements. Time-resolved transient absorption spectroscopy is a convenient way to probe the charge separation and charge transfer processes in CdSe quantum dots as well as confirm the existence of species that exist primarily on the picosecond time scale. In an earlier study we established the size dependence of the electron transfer rate between photoexcited CdSe quantum dots and TiO₂ nanoparticles linked via mercaptopropionic acid in THF suspensions.¹¹ In the current study we subjected CdSe quantum dots deposited on a glass slide and on a TiO₂ nanoparticle film to pump-probe transient absorption spectroscopy. Both films were placed in an airtight quartz sample holder and subjected to a high vacuum environment. The transient spectra recorded following 387 nm laser excitation of the CdSe/Glass and CdSe/MPA/TiO₂ films are shown in Figure 2A,B, respectively. Specifically, Figure 2A,B depicts the difference between the excited-state absorption spectrum and the ground-state absorption spectrum at 1, 10, 100, and 1000 ps after CdSe excitation. While both spectra

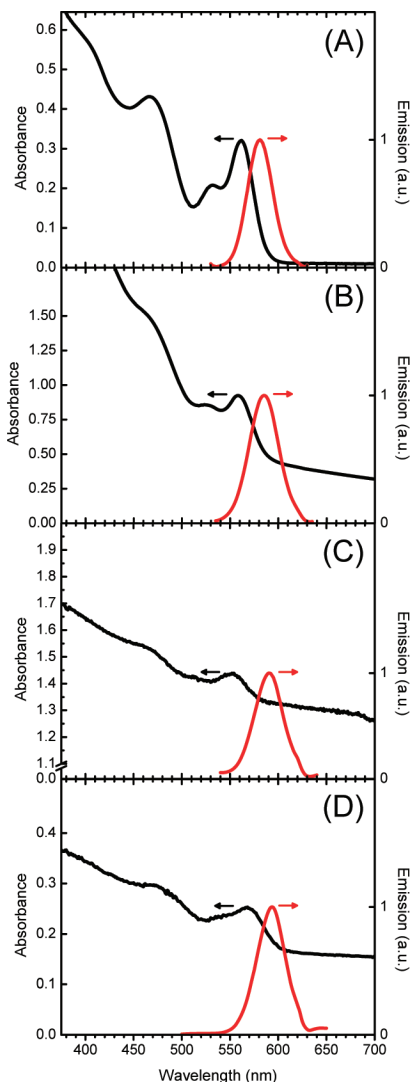


Figure 1. Absorption and emission characteristics of (A) CdSe quantum dots in toluene, (B) CdSe/MPA/TiO₂ film, (C) CdSe/MPS/SiO₂ film, and (D) CdSe dropcast directly on glass. The entirety of this study was carried out using the same batch of CdSe quantum dots.

exhibit a strong bleaching of the CdSe 1S_{3/2}1S_e transition, one additional spectral feature, broad induced absorption, is present in the red-infrared region in the spectrum of the CdSe/MPA/TiO₂ film.

An isosbestic point at 578 nm is also seen in the transient spectra recorded with CdSe/MPA/TiO₂ film, suggesting the

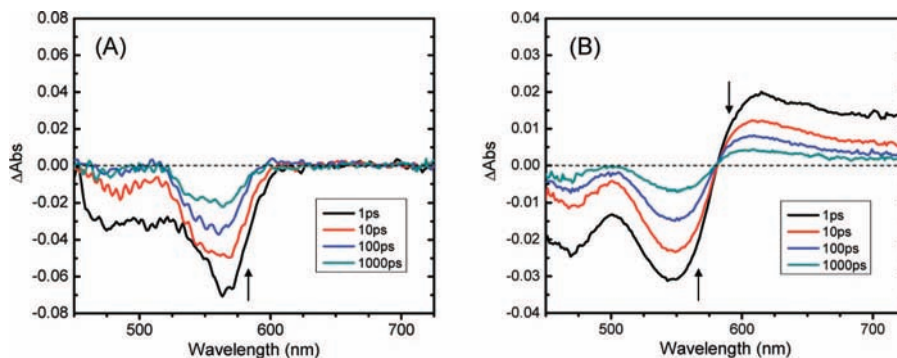
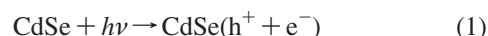


Figure 2. Transient absorption traces at various delay times following 387 nm laser excitation on (A) CdSe/Glass and (B) CdSe/MPA/TiO₂ films in vacuum environment. Arrows are representative of transient trends with increasing delay time.

presence of two states contributing to the transient spectra. The first state, which appears as a bleaching at 550 nm, is assigned to the charge separated state of the CdSe/MPA/TiO₂ composite.²⁷ The formation of the bleaching parallels the appearance of an induced absorption band at ~610 nm. As demonstrated in earlier studies,²⁸ this induced absorption corresponds with the presence of trapped electrons within TiO₂ nanoparticles. As the induced absorption at ~610 nm decreases, the bleaching at ~550 nm recovers, indicating the charge recombination process. Because control experiments consisting of TiO₂ and MPA/TiO₂ nanoparticle films without any anchored CdSe did not yield a transient signal in the picosecond regime, this broad transient of induced absorption in the near-infrared region observed exclusively in the CdSe/MPA/TiO₂ film is indicative of excited-state electron transfer from the CdSe quantum dots to the TiO₂ particles to which they are anchored.

The process of electron injection is initiated when light is absorbed by the CdSe quantum dots to create an electron-hole pair (reaction 1),



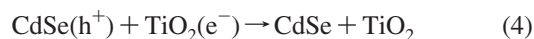
the fate of the electron-hole pair being determined by the substrate to which that quantum dot is anchored. In the case of CdSe/Glass, the fate of the electron-hole pair is limited to recombination (reaction 2):



However, when anchored to a substrate that can readily accept the excited electron, as is the case in CdSe/MPA/TiO₂, electron transfer occurs, leaving behind a hole in the CdSe lattice (reaction 3):



With increasing time most of these injected electrons recombine with holes remaining within neighboring CdSe quantum dots (reaction 4), causing the signal from this particular transient state to be nearly diminished 1000 ps after film excitation.



Given the indication of the presence of electron transfer between CdSe and TiO₂, it would be useful to quantify the rate for this transfer. The experiment described in the following section uses comparative emission lifetime between two films: one in which CdSe dots are anchored to a substrate that will accept excited-state electrons (TiO₂) and one in which they are anchored to a substrate that will not accept excited-state electrons (SiO₂).

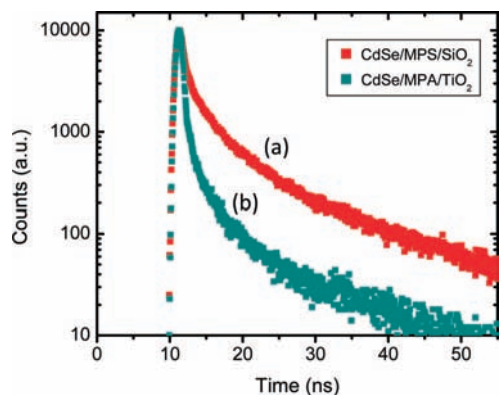


Figure 3. Emission lifetime measurement for both CdSe/MPS/SiO₂ (a) and CdSe/MPA/TiO₂ (b) films. The decrease in CdSe emission lifetime when anchored on TiO₂ is attributed to the additional deactivation pathway of electron transfer to the semiconducting substrate.

Time Resolved Emission Behavior of CdSe on TiO₂ and SiO₂. Since emission decay represents processes responsible for the deactivation of charge separated states, it is useful to compare the time-resolved emission of CdSe/MPA/TiO₂ and CdSe/MPS/SiO₂ films. Films were placed inside of a sample holder, which was then exposed to high vacuum and sealed. The decay traces recorded following laser (457 nm, 1 MHz) excitation are shown in Figure 3. The decays were fit to a double exponential function (see Supporting Information for functional forms). Relevant best-fit parameters are summarized in Table 1.²⁹

Upon bandgap excitation, charge separation is followed by electron–hole recombination to yield emission (reaction 2). When linked to the SiO₂ surface, the emission decay from the quantum dots is due largely to this process. However, when linked to the TiO₂ surface, an enhanced decay rate is evident, and as discussed in our previous study,³⁰ such a faster rate arises from the additional deactivation pathway associated with electron transfer from CdSe into the TiO₂ nanoparticles (reaction 3), which is driven by the energy difference between the conduction bands of CdSe and TiO₂.¹²

If we assume that the electron transfer process is solely responsible for the enhanced emission decay we can obtain an electron transfer rate from expression 5 (see Supporting Information for derivation),

$$k_{\text{ET}} = \frac{1}{\langle \tau \rangle_{\text{TiO}_2}} - \frac{1}{\langle \tau \rangle_{\text{SiO}_2}} \quad (5)$$

where $\langle \tau \rangle_{\text{TiO}_2}$ and $\langle \tau \rangle_{\text{SiO}_2}$ are the weighted average emission lifetimes²⁹ of CdSe quantum dots anchored to TiO₂ and SiO₂, respectively, and take into account both the fast and the slow lifetime components of each respective biexponential fit. By comparing the average lifetimes of CdSe anchored to SiO₂ and TiO₂ we obtained an apparent electron transfer rate constant of $5.62 \times 10^8 \text{ s}^{-1}$. It should be noted that both fast and slow components contribute to the electron transfer. The emission decay monitored in these measurements does not capture ultrafast events (less than 100 ps) because of the laser pulse width and detection time limitations of our apparatus. The electron transfer rate constant reported here is an apparent value and is significantly slower than the ultrafast events seen in the transient absorption measurements.

In a previous study,³⁰ we reported electron transfer rate constants between molecularly linked CdSe quantum dots (diameter 2.4 – 7.5 nm) and TiO₂ nanoparticles in solution to

be in the range of 1.2×10^{10} – $1.0 \times 10^7 \text{ s}^{-1}$, respectively. It is useful at this point to discuss the mechanism behind the electron transfer under investigation. Due to use of mercaptopropionic acid linking molecules, which anchor the CdSe quantum dots to the TiO₂ nanoparticles, along with the lack of conjugation along the carbon backbone within the mercaptopropionic acid family, it appears as though the mechanism for electron transfer is quantum mechanical tunneling between the CdSe and TiO₂ surfaces. Previous studies have been conducted³¹ which estimate the electron transfer mechanism between surface functionalized metal nanoparticles, suggesting three distinct tunneling models: through-bond tunneling, chain-to-chain tunneling, and through-space tunneling. To our knowledge, however, no parallel study has been published to investigate the tunneling mechanism(s) between quantum dots molecularly linked to semiconducting oxides. Therefore, for qualitative discussion purposes we assumed a through-space tunneling model under the WKB approximation to calculate the tunneling rate between two spheres across a 5 Å (the estimation of linker molecule length) long energy barrier of 4.0 eV (the work function of the CdSe conduction band).^{32,33} Full details of this calculation are reported in the Supporting Information. We calculated a tunneling rate constant of $2.1 \times 10^6 \text{ s}^{-1}$, a value which is over 2 orders of magnitude less than the rate constant observed experimentally. This difference is explainable if either the electron transfer under investigation occurs by some mechanism other than tunneling or if the assumed 5 Å intersphere distance is an overestimation of the actual intersphere distance. Due to the lack of conjugation in MPA, we feel that the latter explanation is more plausible.

To further investigate, we also calculated the interparticle distance necessary to produce a tunneling rate equivalent to the electron transfer rate observed experimentally and found that such a rate occurs at a distance of approximately 1.9 Å. Such a distance is indicative of a nonrigid linker molecule which allows the CdSe quantum dot to approach the TiO₂ nanoparticle surface to within a proximity shorter than the overall length of the linker. This concept of a dynamic CdSe/TiO₂ spatial relationship may further contribute to the multiexponential decay observed in the emission lifetime measurement. If the interparticle distance between the electron donor (CdSe) and the electron acceptor (TiO₂) is constantly changing, one would expect emission lifetime measurements made over any appreciable time scale to be a convoluted sample of a range of interparticle distances, thus leading to a range of observed electron transfer rates which are best fit with multiexponential decay models.

Steady-State Photolysis of CdSe Quantum Dot Films. In earlier studies we demonstrated the photoactivity of CdSe quantum dots either by monitoring the photocurrent generation in a photoelectrochemical cell or by carrying out electron transfer reactions.^{34,35} Because of their potential use in solar cell devices one obvious concern is the long-term photostability of the CdSe quantum dot sensitizers. To quantify these stability issues we assembled films of CdSe quantum dots linked to SiO₂ and TiO₂ substrates and subjected them to visible light irradiation ($\lambda > 400 \text{ nm}$, 0.85 W/cm^2) in the absence of a regenerative redox couple. Changes in the film absorption features in both an atmospheric and a vacuum environment were monitored to probe CdSe degradation.

Photoirradiation in an Atmospheric Environment. The absorption spectra recorded following steady-state irradiation of air equilibrated films of CdSe quantum dots on the TiO₂ and SiO₂ surface are shown in Figure 4. Following prolonged photoirradiation of the CdSe/MPA/TiO₂ film, we observed a continuous shift in the absorption edge coupled by an overall

TABLE 1: Result of Double Exponential Fit to Fluorescence Lifetime Measurement^a

	A_1	τ_1	A_2	τ_2	$\langle\tau\rangle$	χ^2
CdSe/MPS/SiO ₂	0.38	9.02×10^{-10} s	0.62	7.00×10^{-10} s	4.70 ns	3.66
CdSe/MPA/TiO ₂	0.80	3.88×10^{-10} s	0.20	4.90×10^{-10} s	1.29 ns	3.30

^a A is the relative amplitude of each lifetime, τ_1 and τ_2 are the fast and slow components of the fluorescence lifetime, respectively, and χ^2 represents the quality of the fit.

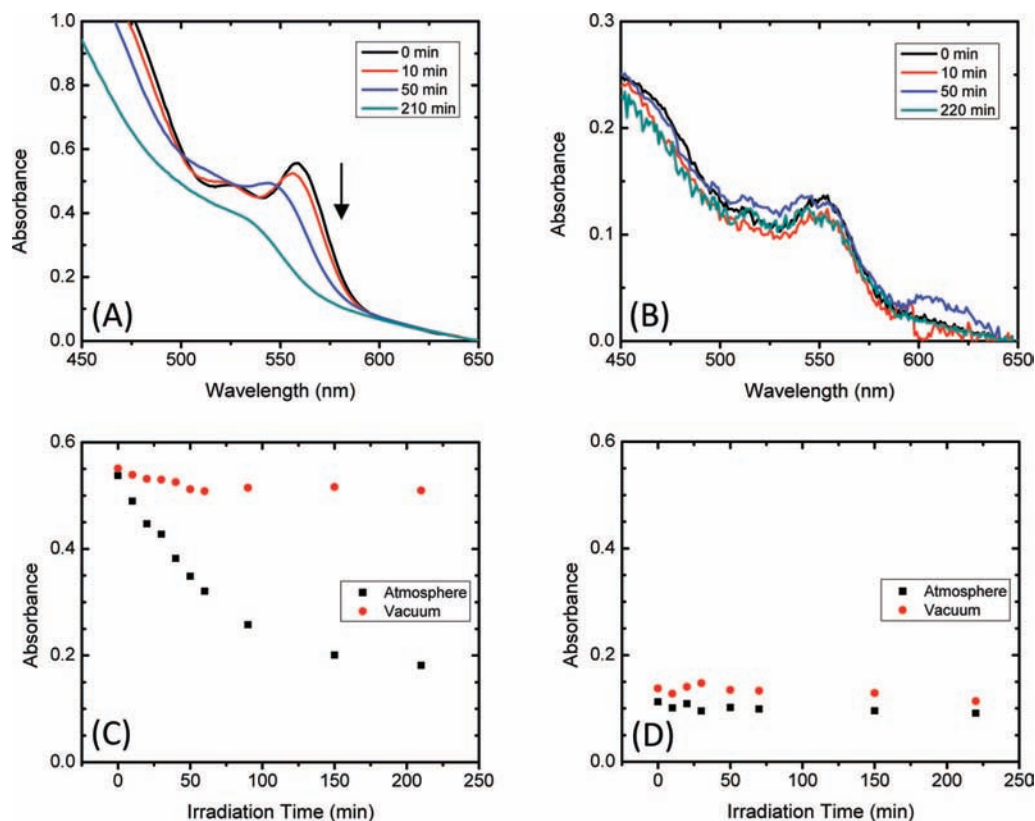


Figure 4. Visible absorption spectra after selected irradiation times for (A) CdSe/MPA/TiO₂ and (B) CdSe/MPS/SiO₂ films exposed to an atmospheric environment. Plot of the absorbance of (C) CdSe/MPA/TiO₂ and (D) CdSe/MPS/SiO₂ films at 562 nm vs irradiation time for films exposed to atmospheric and vacuum environments. Arrow in (A) is representative of absorption trend with increasing irradiation time. For comparison purposes each trace was shifted to zero absorbance at 650 nm to compensate for scattering effects. Unaltered traces are provided in the Supporting Information.

decrease in the $1S_{3/2}1S_c$ transition intensity. Quantitatively, the decrease in absorbance at 562 nm for this film amounted to ~66% during 3.5 h of visible irradiation. In earlier studies, photocorrosion at selective wavelength irradiation was used to decrease the size of CdS particles in suspension.³⁶ To test for the occurrence of photocorrosion in our setup we subjected CdSe/MPS/SiO₂ films to visible irradiation. The quantum dots anchored on an SiO₂ substrate were quite stable and showed only a small change in absorption (decrease of ~19%) during the period of 3.5 h of illumination, suggesting that a CdSe-substrate interaction must play a role in the mechanism for the observed decrease in absorption in the CdSe/MPA/TiO₂ sample, as opposed to direct and exclusive interaction between incident light and CdSe quantum dots.

To further confirm this substrate selective phenomenon visibly we also subjected both TiO₂ and SiO₂ anchored quantum dot films to the same 0.85 W/cm² irradiation source for a period of 4 h each, utilizing a slit (Figure 5) to control the area of each film exposed. Films of quantum dots anchored to both TiO₂ and SiO₂ substrates after slit controlled irradiation are shown in Figure 5. Before photoirradiation both films exhibited strong coloration due to the anchored quantum dot sensitizers; however, after light exposure, the exposed area of the CdSe/MPA/TiO₂

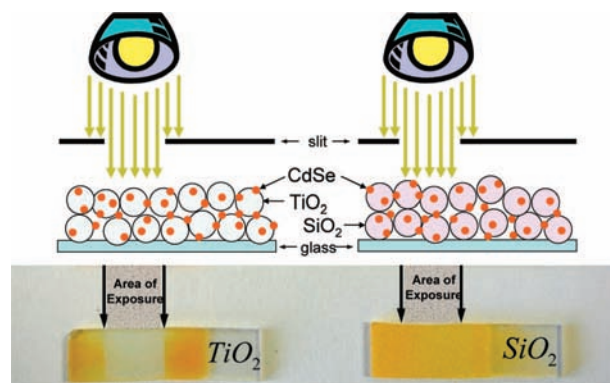
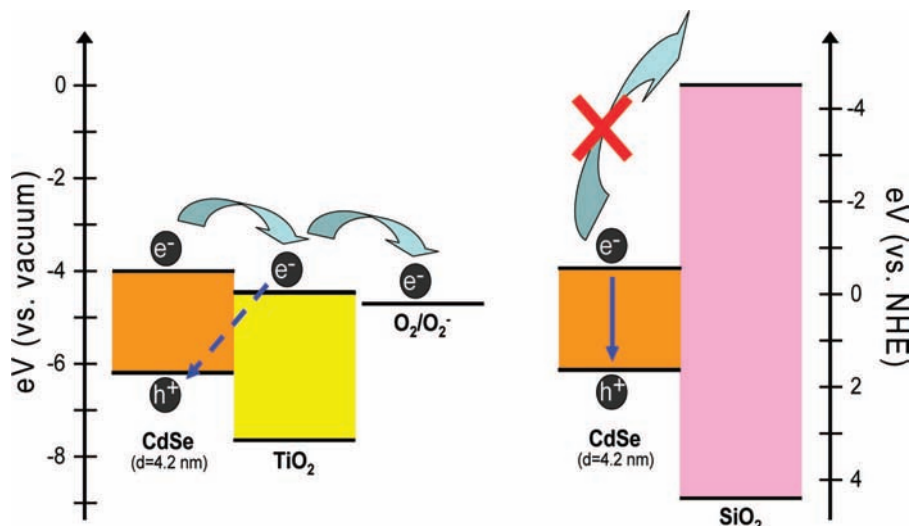


Figure 5. Artistic representation of controlled light exposure to both CdSe/MPA/TiO₂ and CdSe/MPS/SiO₂ films along with a photograph of both after masked irradiation (atmospheric environment).

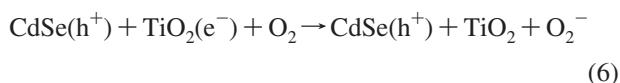
film lost virtually all of its color while the unexposed area appeared nearly unchanged. Conversely, both the exposed and the unexposed areas of the CdSe/MPS/SiO₂ film appeared unchanged. This visual observation further exemplifies the substrate selective nature of CdSe quantum dot photodegradation.

SCHEME 2: Illustration of Band Energies of SiO₂ and TiO₂ in Comparison with CdSe that Influence the Fate of Photogenerated Charge Carriers.^a


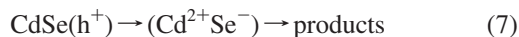
^a States of various species placed on absolute energy scale according to refs 37–41.

Photoirradiation in a Vacuum Environment. When photoirradiation of CdSe/MPA/TiO₂ and CdSe/MPS/SiO₂ films was carried out in an evacuated environment, they did not show significant change in the absorption characteristics. The change in absorbance at 562 nm recorded at different irradiation times for both evacuated and atmosphere equilibrated conditions is shown for TiO₂ and SiO₂ in Figure 4C,D, respectively. Specifically, over a period of 3.5 h of illumination in a vacuum environment the CdSe/MPA/TiO₂ and CdSe/MPS/SiO₂ films showed decreases in absorbance at 562 nm of ~8% and ~17%, respectively. These observations indicate that, in addition to the semiconducting TiO₂ substrate, the presence of O₂ also plays an important role in the photodegradation of CdSe.

Mechanism behind Photodegradation. The mechanism for observed CdSe quantum dot photodegradation (on TiO₂, in air) and stability (on TiO₂, in vacuum; on SiO₂, in vacuum and air) under steady-state visible irradiation is illustrated in Scheme 2.^{37–41} We attribute the photolysis induced absorption changes seen with the CdSe/MPA/TiO₂ sample (air equilibrated) to electron injection from the excited CdSe quantum dot (conduction band energy -4.0 eV vs vacuum for 4.2 nm diameter particle) into the conduction band of TiO₂ (conduction band energy -4.4 eV vs vacuum). In evacuated samples reactions 1–4 dominate as the photogenerated charge carriers undergo recombination to regenerate the CdSe nanocrystallites. In the presence of oxygen, however, electron injection from the CdSe quantum dot to the TiO₂ nanoparticle is followed by the scavenging of the injected electron by surface adsorbed oxygen (reaction 6):



The excess holes remaining in the valence band of the CdSe quantum dots then induce anodic corrosion similar to that reported earlier in both CdS and CdSe colloids⁴² (reaction 7),



where “products” represent the final yield of the oxidation process, the nature of which has been discussed elsewhere.^{43,44}

SiO₂, on the other hand, with its large band gap and near vacuum-level conduction band energy does not participate in

this interparticle electron transfer process because such a transfer would be energetically unfavorable. Hence, in the CdSe/MPS/SiO₂ film, charge carriers generated after CdSe photoexcitation recombine (reaction 2) without participating in surface chemical processes, as charge recombination occurs on a faster time scale than surface O₂/O₂⁻ oxidation. Previously, Nasr et al. observed a similar surface dependent photochemical phenomenon when they anchored a ruthenium(II) polypyridyl complex to both SiO₂ and SnO₂ surfaces.⁴⁵ They found that when compared with SiO₂, the yield of electron transfer products was significantly increased when the complex was anchored to SnO₂, an observation which was attributed to relative energies of the sensitizer and the substrate to which it was anchored.

Further evidence for this mechanism is obtained through the analysis of photochemical changes in CdSe/MPA/TiO₂ and CdSe/MPS/SiO₂ films within evacuated environments. Unlike the film exposed to air, the CdSe quantum dots deposited on TiO₂ remain stable if the photoirradiation is carried out under evacuated conditions (Figure 4C). This stability is attributed to the absence of surface adsorbed oxygen within a high-vacuum environment. Instead of being scavenged by the surface adsorbed oxygen, photogenerated electrons are deactivated through recombination with holes accumulated within the CdSe valence band (reaction 8), which, in turn, prevents anodic corrosion of the CdSe quantum dots.



Figure 4D illustrates that there is no significant degradation of the CdSe within the CdSe/MPS/SiO₂ sample in either the vacuum or the atmospheric environments. These observations rule out direct interaction between photogenerated electrons in CdSe and oxygen. Previously, thin films of CdSe/CdS/ZnS nanocrystals deposited on gold and exposed to either air or nitrogen atmospheres have shown an irreversible quenching of emission when placed under positive bias.⁴⁶ Application of positive bias increases the survivability of holes due to the fact that electrons are swept away from the CdSe nanocrystals. This excess of holes in the CdSe lattice leads to the oxidation of Se²⁻ to generate Cd²⁺Se⁻ within the CdSe matrix, which was

cited as the reason for the observed irreversible quenching of emission. These arguments further support our assessment that the degradation in the present experiment arises from the accumulation of holes within the CdSe structure.

Jasieniak and Mulvaney studied the effect of the Cd to Se surface atom ratio upon the luminescence quantum yield of CdSe quantum dots in solution⁴⁷ and found that, when purged with nitrogen, quantum dots with both Cd-rich and Se-rich surfaces showed strong photostability, but once exposed to an oxygen environment luminescence intensity decreased over the time scale of ~250 min, more drastically so within the solution containing dots with Cd-rich surfaces. In the absence of an adsorbed electron acceptor such as TiO₂ this photodarkening was attributed to the formation of Cd²⁺ species as a result of the oxidation of CdSe by excess holes within the lattice. The present study demonstrates a parallel reduction of 1S_{3/2}1S_e absorption, however, over a shorter time scale of ~45 min compared with the previously discussed work. This comparison highlights the influence of surface adsorbed species on the time scale of CdSe degradation. Specifically, we attribute the increased rate of CdSe corrosion to the electron accepting property of semiconducting TiO₂, where accepted electrons are readily scavenged by oxygen, preventing electron–hole recombination and facilitating hole accumulation within the CdSe lattice.

Implications for CdSe Quantum Dot Based Devices. When constructing a CdSe quantum dot (or dye) sensitized solar cell a critical component is the electrolyte solution, which allows for the replenishment of charge carriers at the electrode surface.⁴⁸ However, when optimizing the performance of such a device one often investigates individual components of that device, that is, the CdSe/MPA/TiO₂ working electrode in the absence of an electrolyte solution. While the degradation we observed in this work could almost certainly be controlled with a proper electrolyte solution, it is important to note that when optimizing individual components of a device—or simply investigating the properties of such films—a vacuum environment is necessary to obtain accurate results and should be implemented in future studies.

These findings also have implications in the study of quantum dot intermittency (blinking). Although great advancements have been made in this area, an explicit mechanism for quantum dot (or molecular) blinking has yet to be reached.⁴⁹ One observed phenomenon, however, is the effect of the surrounding material on blinking statistics. Stefani and co-workers,⁵⁰ for example, observed blinking of Zn_{0.42}Cd_{0.58}Se quantum dots placed on both insulating glass and conducting indium–tin–oxide slides and reported substrate dependent behavior. While the specific mechanism for quantum dot degradation reported within this work does not account for intermittent emission, it may aid in the explanation of the dielectric dependency noted in quantum dot blinking behavior.⁵¹

Conclusion

CdSe quantum dots were anchored on different oxide nanoparticles to investigate the excited-state interactions between those particles and their respective semiconducting substrates. A spectroscopic fingerprint within the transient absorption spectra of CdSe/MPA/TiO₂ demonstrates electron injection from the conduction band of CdSe to the conduction band of TiO₂. The apparent rate constant for electron injection was 5.6×10^8 s⁻¹ as determined from the emission decay of CdSe quantum dots anchored to both TiO₂ and SiO₂. This presence of electron injection allowed us to elucidate a mechanism for the observed

irreversible degradation of CdSe within CdSe/MPA/TiO₂ films in the presence of oxygen. Basic understanding and ultimate control of such photodegradation are crucial for designing new quantum dot/semiconductor based systems as well as the implementation of such systems in commercial devices.

Acknowledgment. The research described herein was supported by the Department of Energy, Office of Basic Sciences. We would like to thank Ian Duncanson for his assistance in creating the sample cells necessary to measure films in high-vacuum environments. We also would also like to thank James Puthussery for his help in synthesizing CdSe quantum dots and Jay Giblin for his helpful discussions regarding the presentation of the tunneling calculation. This is contribution number NDRL 4780 from the Notre Dame Radiation Laboratory.

Supporting Information Available: Irradiation lamp profile, experimental setup used to measure film degradation, emission lifetime fitting equations, outline of quantum mechanical tunneling calculation, and unshifted traces of Figure 4. This material is available free of charge via the Internet at <http://pubs.acs.org>.

References and Notes

- (1) Kamat, P. V. Meeting the clean energy demand: Nanostructure architectures for solar energy conversion. *J. Phys. Chem. C* **2007**, *111*, 2834–2860.
- (2) Peng, X. G.; Manna, L.; Yang, W. D.; Wickham, J.; Scher, E.; Kadavanich, A.; Alivisatos, A. P. Shape control of CdSe nanocrystals. *Nature* **2000**, *404*, 59–61.
- (3) Chan, W. C. W.; Nie, S. M. Quantum dot bioconjugates for ultrasensitive nonisotopic detection. *Science* **1998**, *281*, 2016–2018.
- (4) Goldman, E. R.; Anderson, G. P.; Tran, P. T.; Mattoussi, H.; Charles, P. T.; Mauro, J. M. Conjugation of Luminescent Quantum Dots with Antibodies Using an Engineered Adaptor Protein To Provide New Reagents for Fluoroimmunoassays. *Anal. Chem.* **2002**, *74*, 841–847.
- (5) Medintz, I. L.; Uyeda, H. T.; Goldman, E. R.; Mattoussi, H. Quantum dot bioconjugates for imaging, labeling and sensing. *Nat. Mater.* **2005**, *4*, 435–446.
- (6) Nozik, A. J. Quantum dot solar cells. *Phys. E* **2002**, *14*, 115–120.
- (7) Burda, C.; Chen, X. B.; Narayanan, R.; El-Sayed, M. A. Chemistry and properties of nanocrystals of different shapes. *Chem. Rev.* **2005**, *105*, 1025–1102.
- (8) Krauss, T. D.; Brus, L. E. Electronic properties of single semiconductor nanocrystals: Optical and electrostatic force microscopy measurements. *Mater. Sci. Eng., B* **2000**, *69*, 289–294.
- (9) Scholes, G. D. Insights into excitons confined to nanoscale systems: Electron-hole interaction, binding energy, and photodissociation. *ACS Nano* **2008**, *2*, 523–537.
- (10) Kamat, P. V. Quantum Dot Solar Cells. Semiconductor Nanocrystals as Light Harvesters. *J. Phys. Chem. C* **2008**, *112*, 18737–18753.
- (11) Robel, I.; Subramanian, V.; Kuno, M.; Kamat, P. V. Quantum dot solar cells. Harvesting light energy with CdSe nanocrystals molecularly linked to mesoscopic TiO₂ films. *J. Am. Chem. Soc.* **2006**, *128*, 2385–2393.
- (12) Kongkanand, A.; Tvrdy, K.; Takechi, K.; Kuno, M.; Kamat, P. V. Quantum dot solar cells. Tuning photoresponse through size and shape control of CdSe–TiO₂ architecture. *J. Am. Chem. Soc.* **2008**, *130*, 4007–4015.
- (13) Cohen, H.; Sarkar, S. K.; Hodes, G. Chemically resolved photovoltage measurements in CdSe nanoparticle films. *J. Phys. Chem. B* **2006**, *110*, 25508–25513.
- (14) Peter, L. M.; Wijayantha, K. G. U.; Riley, D. J.; Waggett, J. P. Band-edge tuning in self-assembled layers of Bi₂S₃ nanoparticles used to photosensitize nanocrystalline TiO₂. *J. Phys. Chem. B* **2003**, *107*, 8378–8381.
- (15) Lee, H. J.; Yum, J. H.; Leventis, H. C.; Zakeeruddin, S. M.; Haque, S. A.; Chen, P.; Seok, S. I.; Grazel, M.; Nazeeruddin, M. K. CdSe quantum dot-sensitized solar cells exceeding efficiency 1% at full-sun intensity. *J. Phys. Chem. C* **2008**, *112*, 11600–11608.
- (16) Yu, P. R.; Zhu, K.; Norman, A. G.; Ferrere, S.; Frank, A. J.; Nozik, A. J. Nanocrystalline TiO₂ solar cells sensitized with InAs quantum dots. *J. Phys. Chem. B* **2006**, *110*, 25451–25454.
- (17) Diguna, L. J.; Shen, Q.; Kobayashi, J.; Toyoda, T. High efficiency of CdSe quantum-dot-sensitized TiO₂ inverse opal solar cells. *Appl. Phys. Lett.* **2007**, *91*, 3.
- (18) Gueroui, Z.; Libchaber, A. Single-molecule measurements of gold-quenched quantum dots. *Phys. Rev. Lett.* **2004**, *93*, 4.

- (19) Yu, Y. H.; Protasenko, V.; Jena, D.; Xing, H. L.; Kuno, M. Photocurrent polarization anisotropy of randomly oriented nanowire networks. *Nano Lett.* **2008**, *8*, 1352–1357.
- (20) Savadogo, O. Chemically and electrochemically deposited thin films for solar energy materials. *Sol. Energy Mater. Sol. Cells* **1998**, *52*, 361–388.
- (21) Rodriguez-Viejo, J.; Mattoussi, H.; Heine, J. R.; Kuno, M. K.; Michel, J.; Bawendi, M. G.; Jensen, K. F. Evidence of photo- and electrodarkening of (CdSe)ZnS quantum dot composites. *J. Appl. Phys.* **2000**, *87*, 8526–8534.
- (22) Vinodgopal, K.; Hua, X.; Dahlgren, R. L.; Lappin, A. G.; Patterson, L. K.; Kamat, P. V. Photochemistry of Ru(BPY)₂(DCBPY)₂(2+) on Al₂O₃ and TiO₂ Surfaces - An Insight Into the Mechanism of Photosensitization. *J. Phys. Chem.* **1995**, *99*, 10883–10889.
- (23) Kuno, M. Band Edge Spectroscopy of CdSe Quantum Dots. Ph.D. Thesis, Massachusetts Institute of Technology, Cambridge, MA, 1998.
- (24) Lee, H. J.; Kim, D. Y.; Yoo, J. S.; Bang, J.; Kim, S.; Park, S. M. Anchoring cadmium chalcogenide quantum dots (QDs) onto stable oxide semiconductor for QD sensitized solar cells. *Bull. Korean Chem. Soc.* **2007**, *28*, 953–958.
- (25) Ma, Y.; Li, M. H.; El-Khair, H. M.; Zhang, Y.; Xu, L.; Huang, X. F.; Chen, K. J. Room temperature self-assembly on CdSe nanocrystals on SiO₂-coated Si wafer. *Phys. E* **2002**, *15*, 48–52.
- (26) Norris, D. J. Measurement and Assignment of the Size-Dependent Optical Spectrum in Cadmium Selenide (CdSe) Quantum Dots. Ph.D. Thesis, Massachusetts Institute of Technology, Cambridge, MA, 1995.
- (27) Norris, D. J.; Bawendi, M. G. Structure in the Lowest Absorption Feature of CdSe Quantum Dots. *J. Chem. Phys.* **1995**, *103*, 5260–5268.
- (28) Rothenberger, G.; Moser, J.; Grätzel, M.; Serpone, N.; Sharma, D. K. Charge Carrier Trapping and Recombination Dynamics in Small Semiconductor Particles. *J. Am. Chem. Soc.* **1985**, *107*, 8054–8059.
- (29) James, D. R.; Liu, Y. S.; Demayo, P.; Ware, W. R. Distributions of Fluorescence Lifetimes - Consequences for the Photophysics of Molecules Adsorbed on Surfaces. *Chem. Phys. Lett.* **1985**, *120*, 460–465.
- (30) Robel, I.; Kuno, M.; Kamat, P. V. Size-dependent electron injection from excited CdSe quantum dots into TiO₂ nanoparticles. *J. Am. Chem. Soc.* **2007**, *129*, 4136–4137.
- (31) Slowinski, K.; Chamberlain, R. V.; Miller, C. J.; Majda, M. Through-bond and chain-to-chain coupling. Two pathways in electron tunneling through liquid alkanethiol monolayers on mercury electrodes. *J. Am. Chem. Soc.* **1997**, *119*, 11910–11919.
- (32) Griffiths, D. J. *Introduction to Quantum Mechanics*, 2nd ed.; Pearson Prentice Hall: Upper Saddle River, NJ, 2005.
- (33) Moroz, A. Electron mean free path in a spherical shell geometry. *J. Phys. Chem. C* **2008**, *112*, 10641–10652.
- (34) Dimitrijevic, N. M. Electron-Transfer Reactions on CdSe Colloids as Studied by Pulse-Radiolysis. *J. Chem. Soc., Faraday Trans. I* **1987**, *83*, 1193–1201.
- (35) Chandrasekharan, N.; Kamat, P. V. Tuning the properties of CdSe nanoparticles in reverse micelles. *Res. Chem. Intermed.* **2002**, *28*, 847–856.
- (36) Matsumoto, H.; Sakata, T.; Mori, H.; Yoneyama, H. Preparation of monodisperse CdS nanocrystals by size selective photocorrosion. *J. Phys. Chem.* **1996**, *100*, 13781–13785.
- (37) Bard, A. J.; Faulkner, L. R. *Electrochemical Methods: Fundamentals and Applications*; Wiley: Hoboken, NJ, 2001.
- (38) Van de Walle, C. G.; Neugebauer, J. Universal alignment of hydrogen levels in semiconductors, insulators and solutions. *Nature* **2003**, *423*, 626–628.
- (39) Nozik, A. J.; Memming, R. Physical chemistry of semiconductor-liquid interfaces. *J. Phys. Chem.* **1996**, *100*, 13061–13078.
- (40) Efros, A. L.; Rosen, M. The electronic structure of semiconductor nanocrystals. *Annu. Rev. Mater. Sci.* **2000**, *30*, 475–521.
- (41) Hagfeldt, A.; Grätzel, M. Light-Induced Redox Reactions in Nanocrystalline Systems. *Chem. Rev.* **1995**, *95*, 49–68.
- (42) Dimitrijevic, N. M.; Kamat, P. V. Transient Photobleaching of Small CdSe Colloids in Acetonitrile - Anodic Decomposition. *J. Phys. Chem.* **1987**, *91*, 2096–2099.
- (43) Sears, W. M.; Morrison, S. R. Oxidation Processes on CdSe and Se Electrodes. *J. Phys. Chem.* **1984**, *88*, 976–980.
- (44) Smith, A. M.; Duan, H. W.; Rhyner, M. N.; Ruan, G.; Nie, S. M. A systematic examination of surface coatings on the optical and chemical properties of semiconductor quantum dots. *Phys. Chem. Chem. Phys.* **2006**, *8*, 3895–3903.
- (45) Nasr, C.; Hotchandani, S.; Kamat, P. V. Role of iodide in photoelectrochemical solar cells. Electron transfer between iodide ions and ruthenium polypyridyl complex anchored on nanocrystalline SiO₂ and SnO₂ films. *J. Phys. Chem. B* **1998**, *102*, 4944–4951.
- (46) Gooding, A. K.; Gomez, D. E.; Mulvaney, P. The effects of electron and hole injection on the photoluminescence of CdSe/CdS/ZnS nanocrystal monolayers. *ACS Nano* **2008**, *2*, 669–676.
- (47) Jasieniak, J.; Mulvaney, P. From Cd-rich to Se-rich - The manipulation of CdSe nanocrystal surface stoichiometry. *J. Am. Chem. Soc.* **2007**, *129*, 2841–2848.
- (48) Memming, R. Role of Energy-Levels in Semiconductor-Electrolyte Solar-Cells. *J. Electrochem. Soc.* **1978**, *125*, 117–123.
- (49) Frantsuzov, P.; Kuno, M.; Janko, B.; Marcus, R. A. Universal emission intermittency in quantum dots, nanorods and nanowires. *Nat. Phys.* **2008**, *4*, 519–522.
- (50) Stefani, F. D.; Knoll, W.; Kreiter, M.; Zhong, X.; Han, M. Y. Quantification of photoinduced and spontaneous quantum-dot luminescence blinking. *Phys. Rev. B* **2005**, *72*, 125304–125311.
- (51) Cichos, F.; von Borczyskowski, C.; Orrit, M. Power-law intermittency of single emitters. *Curr. Opin. Colloid Interface Sci.* **2007**, *12*, 272–284.